

Research Article

Electroacupuncture Improves Cognitive Function in Senescence-Accelerated P8 (SAMP8) Mice via the NLRP3/Caspase-1 Pathway

Zhitao Hou ^{1,2}, Ruijin Qiu,² Qingshuang Wei,³ Yitian Liu,³ Meng Wang,¹ Tingting Mei,¹ Yue Zhang,¹ Liying Song,¹ Xianming Shao,¹ Hongcai Shang ², Jing Chen ¹, and Zhongren Sun ^{1,4}

¹College of Basic Medical and Sciences, Heilongjiang University of Chinese Medicine, Harbin, Heilongjiang 150040, China

²Key Laboratory of Chinese Internal Medicine of the Ministry of Education, Dongzhimen Hospital Affiliated with Beijing University of Chinese Medicine, Beijing 100700, China

³School of Acupuncture-Moxibustion and Tuina, Beijing University of Chinese Medicine, Beijing 100029, China

⁴School of Acupuncture-Moxibustion and Tuina, Heilongjiang University of Chinese Medicine, Harbin, Heilongjiang 150010, China

Correspondence should be addressed to Hongcai Shang; shanghongcai@126.com, Jing Chen; chenjing6385@163.com, and Zhongren Sun; 1035186010@qq.com

Received 17 August 2020; Revised 16 October 2020; Accepted 21 October 2020; Published 4 November 2020

Academic Editor: Vincent C. K. Cheung

Copyright © 2020 Zhitao Hou et al. This is an open access article distributed under the Creative Commons Attribution License, which permits unrestricted use, distribution, and reproduction in any medium, provided the original work is properly cited.

Background. Clinically, electroacupuncture (EA) is the most common therapy for aging-related cognitive impairment (CI). However, the underlying pathomechanism remains unidentified. The aims of this study were to observe the effect of EA on cognitive function and explore the potential mechanism by which EA acts on the NLRP3/caspase-1 signaling pathway. **Main Methods.** Thirty male SAMP8 mice were randomly divided into the model, the 2 Hz EA and 10 Hz EA groups. Ten male SAMR1 mice were assigned to the control group. Cognitive function was assessed through the Morris water maze test. Hippocampal morphology and cell death were observed by HE and TUNEL staining, respectively. The serum IL-1 β , IL-6, IL-18, and TNF- α levels were measured by ELISA. Hippocampal NLRP3, ASC, caspase-1, GSDM-D, IL-1 β , IL-18, A β , and tau proteins were detected by Western blotting. **Key Findings.** Cognitive function, hippocampal morphology, and TUNEL-positive cell counts were improved by both EA frequencies. The serum IL-1 β , IL-6, IL-18, and TNF- α levels were decreased by EA treatment. However, 10 Hz EA reduced the number of TUNEL-positive cells in the CA1 region and serum IL-1 β and IL-6 levels more effectively than 2 Hz EA. NLRP3/caspase-1 pathway-related proteins were significantly downregulated by EA, but 2 Hz EA did not effectively reduce ASC protein expression. Interestingly, both EA frequencies failed to reduce the expression of A β and tau proteins. **Significance.** The effects of 10 Hz EA at the GV20 and ST36 acupoints on the NLRP3/caspase-1 signaling pathway may be a mechanism by which this treatment relieves aging-related CI in mice.

1. Introduction

Cognitive impairment (CI) is a common neurological disease among the elderly [1]. With the rapid aging of the global population, the proportion of patients with CI has been increasing year by year [2]. Current studies have found that the prevalence of dementia is 1% in people over 60 years old and more than 40% in people over 85 years old [3, 4]. Although the exact pathogenesis of CI is not yet clear, hippocampal pyroptosis induced by the chronic inflammatory cascade has been proposed by many scholars [5–7].

Pyroptosis is a new mechanism of cell death discovered in recent years. Caspase-1-mediated cell pyroptosis is a classical pathway that can be caused by chronic inflammation in aging [8]. Caspase-1-mediated cell pyroptosis is accompanied by the release of a large number of proinflammatory factors, which induces a cascade of amplified inflammatory responses, and staining reveals that the nuclear DNA undergoes changes similar to those that occur in cell apoptosis [9]. The major difference between caspase-1-mediated cell pyroptosis and cell apoptosis is that in the former process the cell membrane is destroyed, the cell swells due to increased

permeability, and the contents of the cell are released to the extracellular environment [9, 10]. Furthermore, NOD-like receptor protein 3 (NLRP3), apoptosis-associated speck-like protein containing a CARD (ASC), and cysteinyl aspartate-specific protease-1 (caspase-1) are activated, forming the NLRP3 inflammasome [11]; additionally, the production of interleukin- (IL-) 1β and IL-18 is induced [12]. Then, the downstream signaling pathways are activated, promoting inflammation and inducing neural plasticity damage and other neuronal damage [13].

Electroacupuncture (EA) is commonly used as a clinical rehabilitation therapy to improve cognitive dysfunction. Two main EA frequencies are commonly used, namely, low frequency (2 Hz) and high frequency (10 Hz), both of which can effectively improve indexes of clinical outcomes [14]. EA can effectively reduce the levels of interleukin- 1β (IL- 1β), interleukin-6 (IL-6), interleukin-18 (IL-18), and tumor necrosis factor- α (TNF- α), helping to inhibit the inflammatory response in a variety of neurological diseases [15–17]. This study is aimed at revealing the potential mechanism by which different frequencies of EA improve cognitive function by inhibiting pyroptosis of the hippocampus in SAMP8 mice; the underlying goal is to provide new therapeutic ideas for a rational selection of EA therapy as an intervention in clinical and basic research on cognitive impairment.

2. Materials and Methods

2.1. Animals and Ethics Statement. Seven-month-old male senescence-accelerated P8 (SAMP8) mice and senescence-resistant R1 (SAMR1) mice were purchased from the experimental animal center of the First Affiliated Hospital of Tianjin University of Chinese Medicine (Tianjin, China). The experiment was conducted in accordance with the laboratory animal use regulations of the Animal Care and Use Committee of Heilongjiang University of Chinese Medicine. All animals were housed in a specific-pathogen-free room (20~22°C, 40%~60% humidity) under a 12 h day/night cycle with sterile feed and autoclaved water ad libitum. After 7 days of adaptation to the new environment, all animals underwent the formal experiment.

2.2. Animal Grouping and Administration. Ten SAMR1 mice (7 months old, 22~25 g) were assigned to a control group ($n = 10$; day 0) that received no intervention. Thirty SAMP8 mice with CI (7 months old, 22~25 g) were randomly divided into three groups ($n = 10$ each; days 0, 1): a model group, which received no intervention; (2) a low-frequency EA group, which received EA (1 mA, 2 Hz) for 30 min once daily for 14 consecutive days; and (3) a high-frequency EA group, which received EA (1 mA, 10 Hz) for 30 min once daily for 14 consecutive days. Seven days before grouping and interventions, all mice underwent Morris water maze (Biobserve, Bonn, Germany) cued training tests to select for mice with CI. The criterion for selecting mice with CI was a significantly prolonged escape latency (>80 s) according to our previous study [18]. After the EA intervention ended, the mice were tested with the Morris water maze to evaluate the cognitive ability of each group. Samples of hippocampal tissue and

serum were collected for further evaluation after cognitive function assessment. Neuropathological staining was performed by HE staining, and dead cells were stained with the terminal deoxynucleotidyl transferase-mediated dUTP nick-end labeling (TUNEL) method. Enzyme-linked immunosorbent assays (ELISAs) were used to detect the serum levels of IL- 1β , IL-6, IL-18, and TNF- α . Western blotting was used to detect the expression levels of NLRP3, ASC, caspase-1, GSDM-D, IL- 1β , IL-18, tau and A β (Figure 1).

2.3. EA Treatment. The mice from the two EA groups were fixed in a prone position with a stereotaxic device. The acupuncture needles (0.3 mm diameter, Guizhou Ande Medical Appliances, Ltd.) were inserted at a depth of 2-3 mm into the Baihui acupoint (GV20) and Zusanli acupoint (ST36), and then, a Great Wall Acupoint Nerve Stimulator (Model: KWD-808I, Changzhou Wujin Great Wall Medical Equipment Co., Ltd., Changzhou, China) was used. The control and model groups did not receive any EA treatment.

2.4. Cognitive Function Assessment. Cognitive function was assessed 7 days before EA administration by the Morris water maze test to select for mice with CI. The Morris water maze comprises two pieces of equipment: a circular pool and an automatic video analysis system for movement tracking and recording. The circular pool had a diameter of 200 cm and a height of 80 cm and was divided into four black quadrants. Different color stickers were placed above the inner walls of different quadrants. All animals performed 4 trials/day with 10 min intertrial intervals and a maximum trial duration of 90 s. Each mouse was allowed to remain on the platform for 30 s at the end of each trial, and a visible circular platform was placed in a different quadrant 1.5 cm above the water for each trial. The criterion for selecting mice with CI was a significantly prolonged escape latency (>80 s) before animal grouping and EA administration according to our previous study [18].

After EA administration ended, cognitive function was assessed in each group mice once per day for six consecutive days. This test was mainly divided into two aspects: (1) a navigation experiment conducted on the first five consecutive days to measure the learning ability of the mice during which each group of mice was placed into the water at a fixed position in the first quadrant, and the position and movement track of the mice in the water were recorded in real time with a high-speed camera. The assessment indexes were escape latency (seconds), the distance travelled (mm), speed (mm/s), and the time required for the mice to find and climb onto the platform. The maximum swimming time was set at 120 seconds. The time to reach the platform, travelling distance, and speed were observed and recorded. If an animal did not find the platform within 120 seconds, it was led to the platform, and the escape latency was recorded as 120 seconds. Then, the distance travelled and speed were recorded. (2) A space exploration experiment conducted on the 6th day to measure the ability of the mice to maintain long-term memories during which the platform was removed, and the number of times that the mice crossed the location where the platform had been was calculated as the

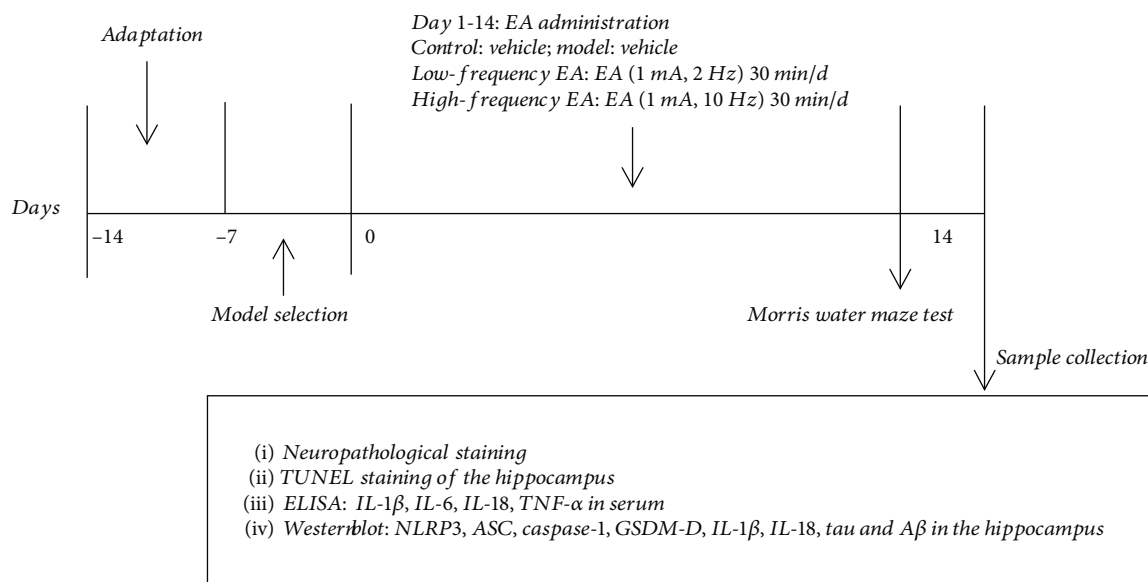


FIGURE 1: Experimental procedures.

assessment index. During the experiment, all groups, including the control group, underwent the above tests. The laboratory environment was kept quiet, the water temperature was maintained at 22~26°C, and the light and objects around the water maze pool remained unchanged to reduce experimental errors caused by interference from the external environment. After each experiment, the pool was cleaned, the hair of the mice was dried, and the mice were given free access to food and water in accordance with the ethical requirements of animal welfare guidelines.

2.5. Neuropathological Staining. The mice were anesthetized with isoflurane gas anesthesia using a small animal anesthesia machine (Shanghai Sango Biotechnology Co., Ltd., Shanghai, China) after the final Morris water maze assessment. The brain tissues of the mice were placed in phosphoric acid buffer (PB) containing 4% paraformaldehyde and then fixed for 24 h. The tissues were embedded in paraffin and cut into continuous coronal sections. The slices were routinely dewaxed with dimethyl benzene and then rehydrated with the following alcohol series: xylene (I) 5 min, xylene (II) 5 min, anhydrous ethanol (I) 2 min, anhydrous ethanol (II) 2 min, 95% ethanol (I) 2 min, 95% ethanol (II) 2 min, and 80% ethanol 1 min. The slides were washed with distilled water for 1 min. Hematoxylin stain was applied for 5 min and rinsed away with tap water for 1 min. Next, 1% HCl ethanol was applied for 3 s for differentiation, and the samples were washed for 2 s; blue (with warm water or 1% ammonia, etc.) was applied for 10 s followed by a water rinse for 1 min, rinsing with distilled water for 1 min, and staining with 0.5% eosin for 2 min. Conventional dehydration, clearing, and sealing were performed. We selected 1 slice at intervals of 10 slices, the slice thickness was 4 μ m, and a total of 10 slices were selected for observation. Microscopy (OPTEC, BK-DM320/500, Germany) at 400, 800, and 1600x magnification was used to observe and photograph changes in the pathological structure of the hippocampal CA1 and CA3 regions.

2.6. TUNEL Staining. Paraffin sections of hippocampal tissues were washed with PBS, and the sections were placed in a DNase-free protease K solution of 20 g/mL and incubated at room temperature for 30 min. The specimens were washed with PBS for 5 min 3x, and then, 3% H₂O₂ solution was added for 10 min of room temperature incubation to eliminate endogenous peroxidase activity. The sections were permeabilized in PBS solution containing 0.1% Triton X-100 for 15 min. Then, a TUNEL detection solution containing TdT enzyme and biotin was drizzled onto the section and incubated in darkness at 37°C for 60 min. After the tissue was washed with PBS, the stop solution was applied dropwise to the sections, which were then incubated at room temperature for 10 min. The sections were washed with PBS for 5 min 3x; then, streptavidin-HRP working fluid was applied dropwise, and the sections were incubated at room temperature for 30 min. After 3 washes in PBS for 5 min each, DAB chromogen was applied dropwise to the sections, and they were incubated at room temperature for 10 min. The slices were washed with PBS for 5 min 3x, and nuclear staining was conducted with hematoxylin staining solution. Finally, the specimens were washed with PBS for 5 min 3x and sealed for observation. Five uncrossed and repeated fields were selected from each pathological section under an optical microscope, and cells with brown-yellow particles in the cytoplasm were regarded as positive apoptotic cells. We selected 1 slice at intervals of 10 slices, the slice thickness was 4 μ m, and a total of 10 slices were selected for observation. Ten fields per image were randomly selected to calculate the mean number of TUNEL-positive cells. ImagePro Plus 6.0 pathological image analysis software (Media Cybernetics, Inc., Rockville, MD, USA) was used to calculate the number of TUNEL-positive cells, and the average value was taken as the number of positive cells in the sample: TUNEL – positive cells ratio (%) = number of positive apoptotic cells / (number of positive apoptotic cells + number of negative apoptotic cells) \times 100%.

2.7. ELISA. At the end of the experiment, eyeballs were removed for blood collection. The serum was separated by centrifugation at 3300 r/min at 4°C for 10 min, stored in a refrigerator at -80°C, and then used to measure the serum IL-1 β , IL-6, IL-18, and TNF- α levels. Using an ELISA kit (Nanjing Jiancheng Bioengineering Institute, Nanjing, China), the IL-1 β , IL-6, IL-18, and TNF- α levels were measured following the manufacturer's instructions.

2.8. Western Blotting. The frozen mouse hippocampal tissue in the -80°C refrigerator was taken out and thawed. The hippocampus was separated, transferred to an Eppendorf tube, and cut into pieces as much as possible with special scissors, and then, 50 mg of brain tissue was mixed with 300 μ L of RIPA lysate according to the instructions of the protein extraction reagent kit (Elabscience Biotechnology Co., Ltd., Wuhan, China). Then, 50 μ g of protein from each group was transferred to PVDF membranes (Thermo Fisher Scientific) and blocked with 5% nonfat milk overnight at 4°C. After washing, the membranes were incubated with the following primary antibodies: NLRP3 (rabbit polyclonal, 1:1000, Cell Signaling Technology, Danvers, MA, USA), ASC (rabbit polyclonal, 1:1000, Cell Signaling Technology, Danvers, MA, USA), GSDM-D (rabbit polyclonal, 1:1000, Cell Signaling Technology, Danvers, MA, USA), Caspase-1 (rabbit polyclonal, 1:1000, Cell Signaling Technology, Danvers, MA, USA), IL-1 β (rabbit polyclonal, 1:1000, Cell Signaling Technology, Danvers, MA, USA), IL-18 (rabbit polyclonal, 1:1000, Cell Signaling Technology, Danvers, MA, USA), Tau (rabbit polyclonal, 1:1000, Cell Signaling Technology, Danvers, MA, USA), and A β (rabbit polyclonal, 1:1000, Cell Signaling Technology, Danvers, MA, USA). The membranes were subsequently sealed for incubation with the antibodies. AB luminescent solution (Beijing Prilett Co., Ltd., Beijing, China) was used for development and exposed onto the imaging system (Kodak, Rochester, NY, USA). Strip gray scale analysis was performed with ImageJ software (National Institutes of Health, Bethesda, MD, USA) and seven samples in each group.

2.9. Statistical Analysis. SPSS 22.0 (SPSS Inc. Chicago, IL, USA) and GraphPad Prism 8.0.1 (GraphPad Software Inc., San Diego, CA) software were used for statistics and mapping. Data were presented as the mean \pm standard deviation. All data were collected and analyzed in a blinded manner. Using one-way analysis of variance (ANOVA), two-way ANOVA or two-way repeated-measures ANOVA followed by Bonferroni's post hoc test, we analyzed the escape latency, distance travelled, swimming speed, and target platform crossing number in the Morris water maze test. The Student-Newman-Keuls test was also used for multiple comparisons. Student's *t*-test (two-group comparison) was performed for intergroup comparisons under the condition of a normal distribution and homogeneity of variance. A nondifferential test was used when the variances were uneven. $P < 0.05$ was considered statistically significant.

3. Results

3.1. EA Treatment at the GV20 and ST36 Acupoints Improved Cognitive Function in SAMP8 Mice. We applied two different

frequencies of EA treatment to SAMP8 mice for 14 days to determine whether stimulation at the GV20 and ST36 acupoints can protect against cognitive dysfunction. Two aspects of cognitive function were assessed (Figures 2(a)–2(e)). Significantly prolonged escape latency and a longer distance travelled were observed for the SAMP8 mice in the model group compared with those in the control group ($P < 0.01$). The escape latency and distance travelled of the SAMP8 mice were significantly decreased after 14 days of EA treatment at both frequencies ($P < 0.01$). No direct evidence indicated the frequency at which EA more effectively reduced escape latency and the distance travelled ($P > 0.05$) (Figures 2(a) and 2(b)). Typical swimming trajectories of the mice in each group in the first five days are shown in Figure 1(e). During the experiment, no significant difference in swimming speed was observed between each group ($P > 0.05$) (Figure 2(c)), indicating that the test frequency did not cause exhaustion and that the motor function of the model animals was not damaged. On the other hand, we found that compared with the control group the number of target platform crossings in the model group decreased significantly ($P < 0.01$), and 14 days of consecutive EA treatment could effectively improve the crossing times of the SAMP8 mice. No direct evidence indicates the frequency at which EA was more effective ($P > 0.05$) (Figure 2(d)).

3.2. EA Treatment at the GV20 and ST36 Acupoints Alleviated Hippocampal Neuropathological Injury in SAMP8 Mice. HE staining showed that the neurons in the hippocampal CA1 and CA3 regions of SAMR1 mice in the control group had complete, clearly, and orderly structures, and no abnormalities were observed. In the model group, pyramidal cells in the hippocampal CA1 and CA3 regions were sparse, and the gaps increased. Obvious pathological, morphological, and structural changes (black arrow) were mainly observed: cell boundaries were unclear, cell body swelling increased, and nuclear shrinkage migrated. The pathological changes in neurons in the hippocampal CA1 and CA3 regions in the 2 Hz EA and 10 Hz EA groups were alleviated to a certain degree compared with those in the model group (black arrow), and the effects were the most significant in the 10 Hz EA group, with an orderly arrangement of neurons, clear cell boundaries, and a small number of morphological and structural abnormalities of neurons (black arrow) (Figure 3).

3.3. EA Treatment at the GV20 and ST36 Acupoints Reduced Cell Death in the Hippocampal Neurons of SAMP8 Mice. TUNEL-positive cells were identified by a brown-yellow lesion structure (black arrow) (Figure 4(a)). The number and ratio of TUNEL-positive neurons in the hippocampal CA1 and CA3 regions in the model group were significantly increased compared with those in the control group (Figures 4(b) and 4(c)) ($P < 0.001$), and the number and ratio of TUNEL-positive neurons in the hippocampal CA1 and CA3 regions in the 2 Hz EA and 10 Hz EA groups were significantly decreased compared with those in the model group (Figures 4(b) and 4(c)) ($P < 0.01$). Compared with EA at

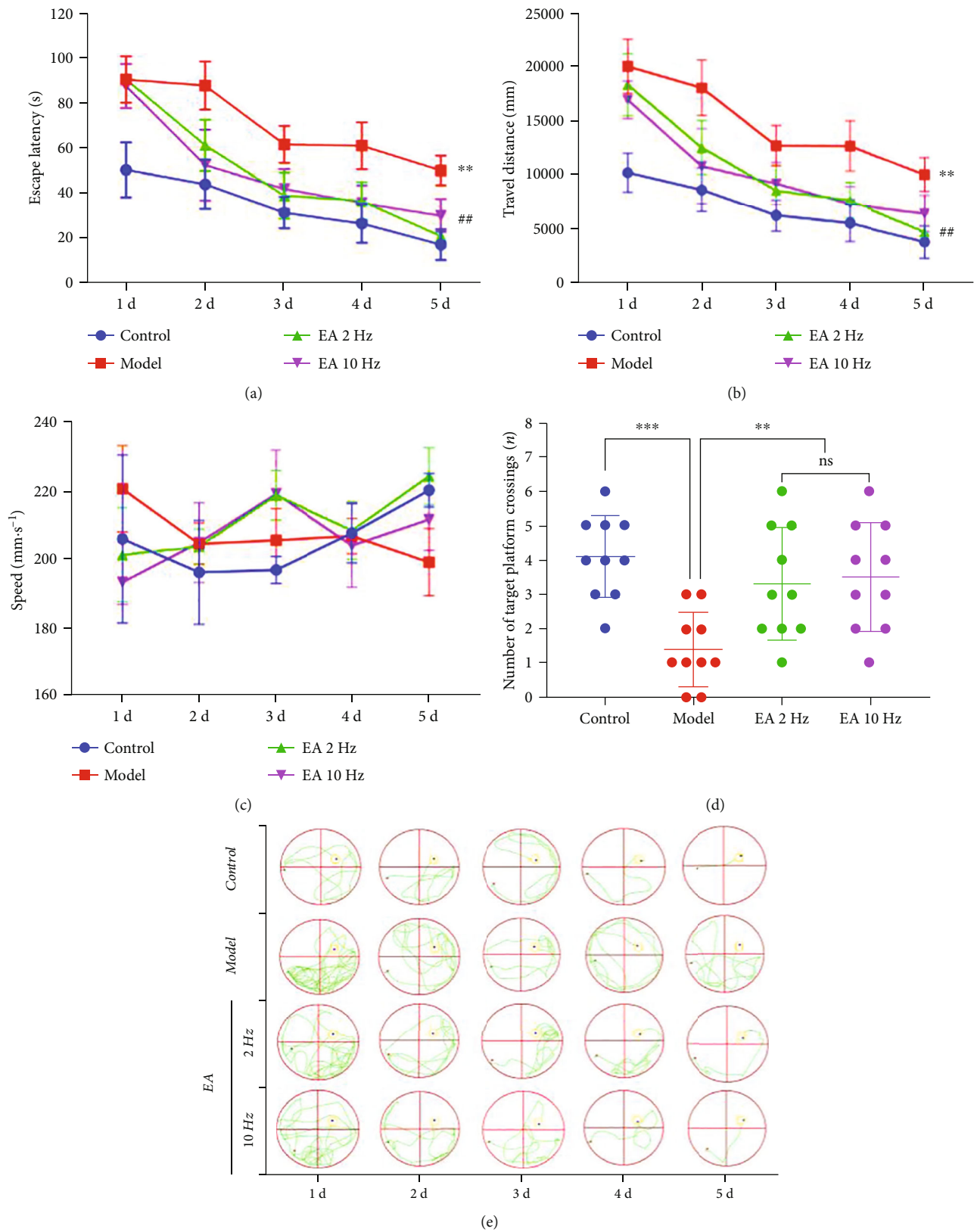


FIGURE 2: Electroacupuncture (EA) treatment enhanced learning and memory abilities in SAMP8 mice in two different cognitive function assessment experiments. (a) The escape latency in the navigation experiment. (b) The distance travelled in the navigation experiment. (c) The speed in the navigation experiment. (d) The target platform crossing number in the space exploration experiment. (e) The typical swimming trajectories in the navigation experiment. The data are shown as the mean \pm SD of 10 mice per group. *** $P < 0.001$ and ** $P < 0.01$ vs. the model group; ## $P < 0.01$ vs. the 2 Hz EA group. ns: not significant.

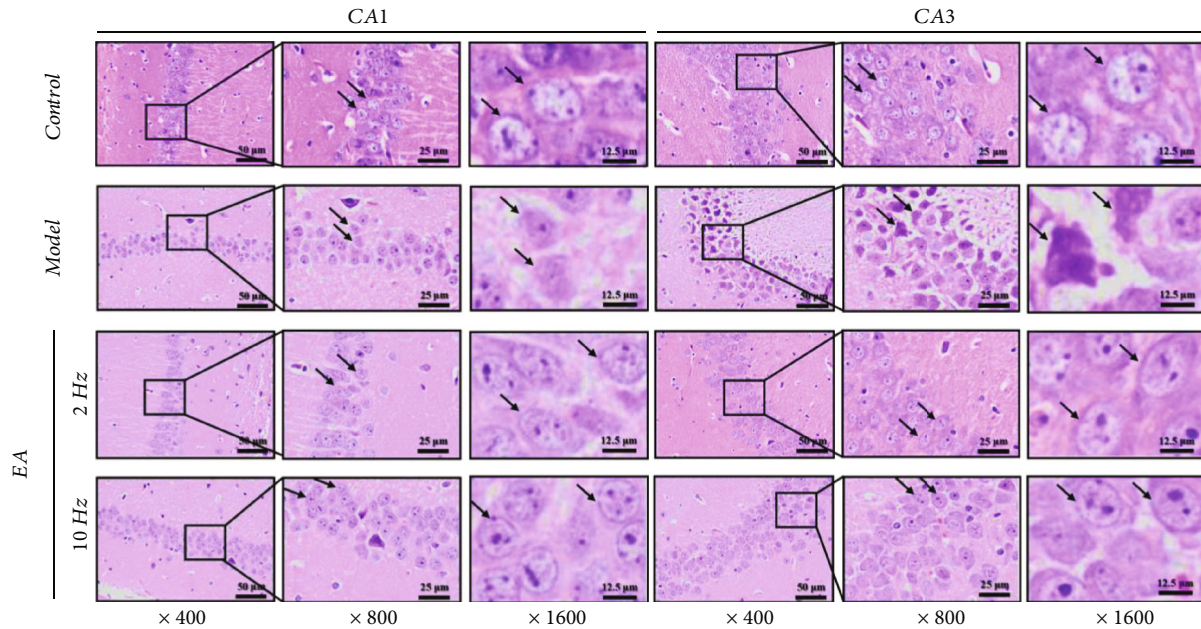


FIGURE 3: Electroacupuncture (EA) treatment was neuroprotective in the hippocampal CA1 and CA3 regions of SAMP8 mice. Magnification times, $\times 400$, $\times 800$, and $\times 1600$. Bar, $50 \mu\text{m}$, $25 \mu\text{m}$, and $12.5 \mu\text{m}$.

2 Hz, EA at 10 Hz can effectively reduce the number and ratio of positive cells in the CA1 region (Figure 4(b)) ($P < 0.05$).

3.4. EA Treatment at the GV20 and ST36 Acupoints Decreased Serum Inflammatory Factor Levels in SAMP8 Mice. We detected the levels of four common inflammatory factors, IL-1 β , IL-6, IL-18, and TNF- α , in the serum of mice and found that compared with the control group the levels of four inflammatory factors in the model group were significantly increased ($P < 0.001$). After 14 days of EA treatment, the levels of four inflammatory factors decreased significantly ($P < 0.001$ or $P < 0.01$) (Figures 5(a)–5(d)). Compared with 2 Hz EA therapy, 10 Hz EA significantly reduced the levels of IL-1 β and IL-6 ($P < 0.05$) (Figures 5(a) and 5(b)).

3.5. EA Treatment at the GV20 and ST36 Acupoints Acted via the NLRP3/Caspase-1 Pathway to Improve Cognitive Function in SAMP8 Mice. We measured the expression of 8 proteins, including NLRP3, ASC, caspase-1, GSDM-D, IL-1 β , IL-18, A β , and tau, in the hippocampal tissues of mice and found that compared with the control group the model group had increased expression of 7 proteins (all but tau; $P < 0.001$ for each comparison). Compared with the model group, the expression of 5 proteins, including NLRP3, caspase-1, GSDM-D, IL-1 β , and IL-18, was significantly decreased after 14 days of 2 Hz EA treatment ($P < 0.001$). After 14 days of 10 Hz EA treatment, the expression of 6 proteins, including NLRP3, ASC, caspase-1, GSDM-D, IL-1 β , and IL-18, was significantly decreased compared with the model group ($P < 0.001$). Compared with the 2 Hz EA group, the expression of 5 proteins, NLRP3, ASC, caspase-1, IL-1 β , and IL-18, in the 10 Hz group was significantly downregulated ($P < 0.05$ or $P < 0.01$) (Figures 6(a)–6(i)). Interestingly,

EA (2 Hz and 10 Hz) treatment had no significant effect on the expression of A β and tau proteins in the hippocampal tissues of SAMP8 mice, and the difference was not significant ($P > 0.05$) (Figures 6(a) and 6(h)–6(i)).

4. Discussion

The purpose of our study was to investigate whether SAMP8 mice with CI would benefit from different frequencies of EA treatment commonly used in clinical and previous studies [19, 20] and to explore the underlying mechanism based on NLRP3/caspase-1-mediated hippocampal pyroptosis induced by the chronic inflammatory cascade. The findings clearly suggest that EA treatment does have the hypothesized effect.

4.1. EA Is an Effective Therapy for Cognitive Impairment Caused by Aging. In recent years, a growing amount of evidence has confirmed EA as an effective therapy for a wide variety of diseases featuring cognitive dysfunction, such as Alzheimer's disease (AD) [21], vascular dementia (VD) [22], and CI [23, 24]. For example, EA treatment at the GV20 and ST36 acupoints improves model animal learning and memory abilities and protects against hippocampal injury, inhibits inflammatory factors, and regulates brain activity via antioxidative damage [25, 26]. An increasing number of countries have endorsed the efficacy and safety of EA treatment [27, 28]. These considerations led us to further explore the potential improving cognitive effects of EA treatment on CI in our SAMP8 mouse model.

In this study, we found that EA treatment at the GV20 and ST36 acupoints improved cognitive function in SAMP8 mice. According to our previous studies and other reports in the literature [18, 29], 7-month-old SAMP8 mice showed

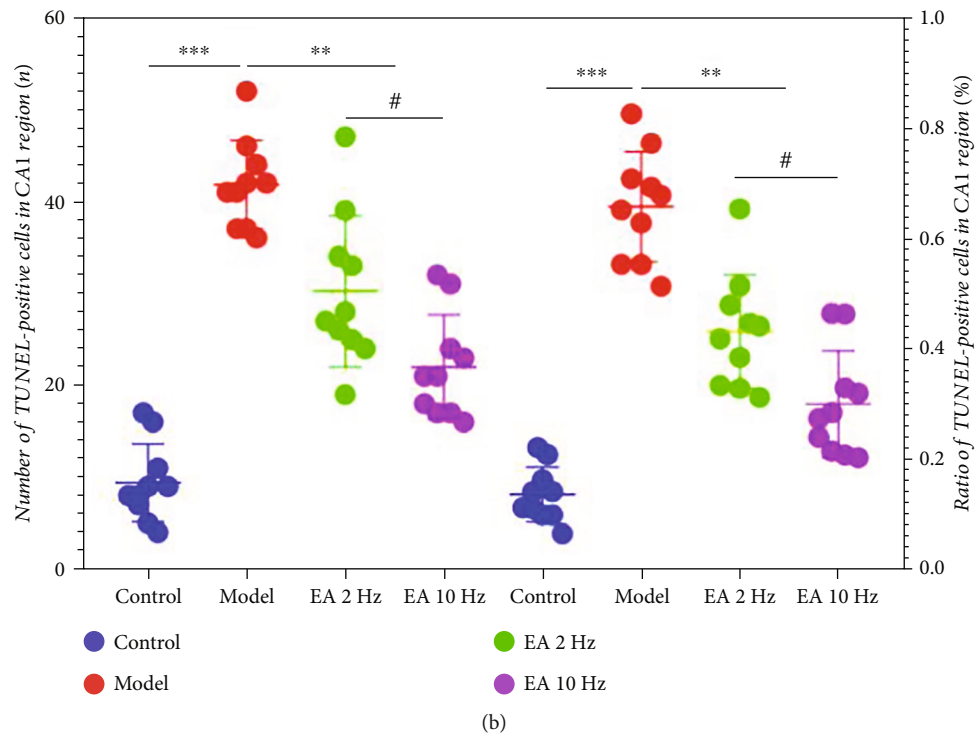
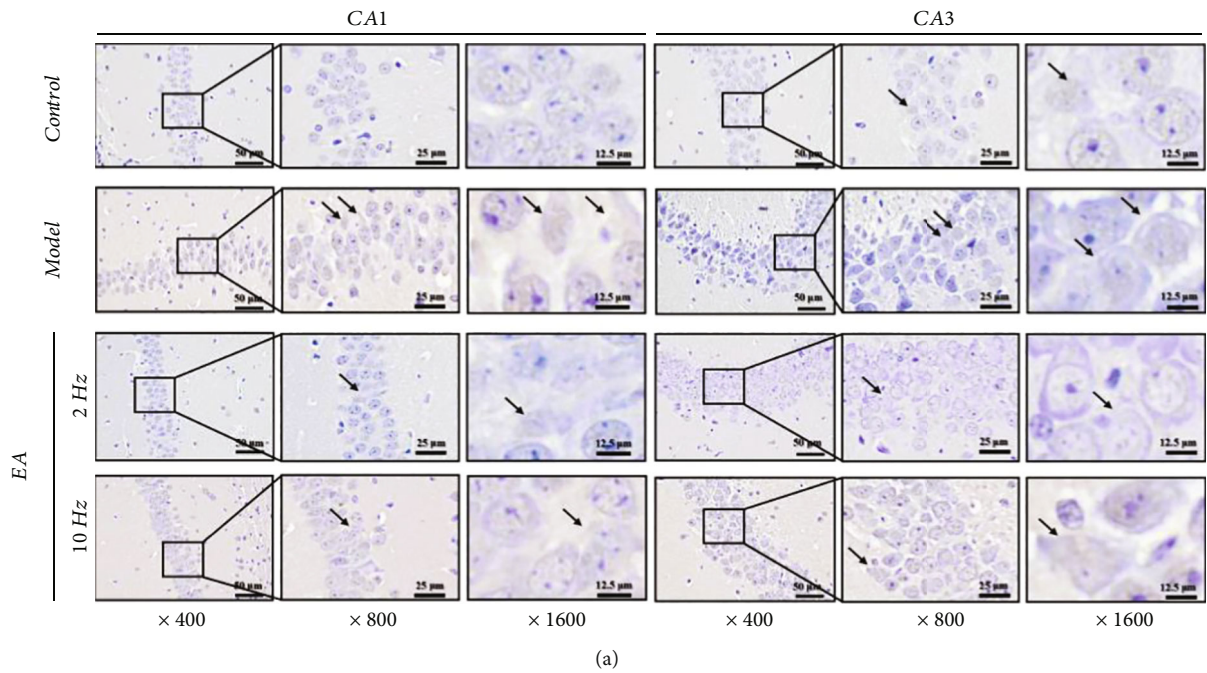


FIGURE 4: Continued.

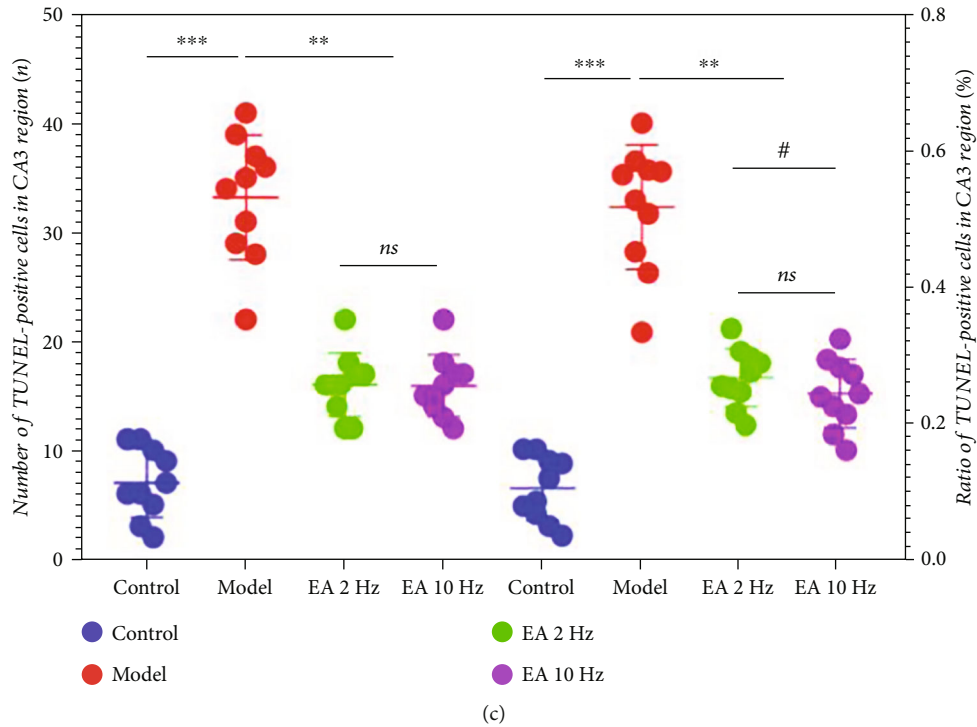


FIGURE 4: Electroacupuncture (EA) treatment limits neuronal cell death in the hippocampal CA1 and CA3 regions in SAMP8 mice. (a) Representative images of TUNEL staining in the hippocampal CA1 and CA3 regions from SAMR1 or SAMP8 mice. Magnification, $\times 400$, $\times 800$, and $\times 1600$. Scale bars, $50 \mu\text{m}$, $25 \mu\text{m}$, and $12.5 \mu\text{m}$. (b) The number and ratio of TUNEL-positive cells in the CA1 region. (c) The number and ratio of TUNEL-positive cells in the CA3 region. Data are the mean \pm SD ($n = 10$ per group). *** $P < 0.001$ and ** $P < 0.01$ vs. the model group; # $P < 0.05$ vs. the 2 Hz EA group. ns: not significant.

significant CI, and SAMR1 mice of the same age were selected as controls. Both animals are ideal models for studying CI induced by aging and are also ideal animal models for drug screening and treatment evaluation [30]. After 14 days of EA treatment, the learning ability of the animals in each group was investigated by navigation experiments for 5 consecutive days. EA at low (2 Hz) and high (10 Hz) frequencies effectively reduced the escape latency and travel distance of SAMP8 mice and resulted in clearer swimming tracks. Compared with the 2 Hz EA treatment, the 10 Hz EA treatment improved the learning ability of SAMP8 mice more significantly, but the difference was not significant ($P > 0.05$). On the sixth day, a spatial exploration experiment was conducted to investigate the memory ability of the animals in each group. EA at both frequencies effectively improved the crossing times of the target platform of SAMP8 mice, but no significant difference was found between the EA groups ($P > 0.05$). In the Morris water maze experiment, we did not observe significantly decreased swimming speed due to physical exhaustion and other factors during 6 consecutive days of testing, indicating that the Morris water maze is safe and reliable as a behavioral standard for evaluating the cognitive function of animals, and the experimental results will not be affected if each group is under the same experimental conditions. The above evidence suggests that EA treatment at either frequency can effectively improve the cognitive function of SAMP8 mice.

4.2. Increase in EA Frequency Plays a Better Role in Inhibiting Inflammation and Hippocampal Cell Death. The chronic inflammatory cascade reaction induced by aging is the main factor stimulating the death of hippocampal neurons. Our previous study found that IL-1 β , IL-6, IL-18, and TNF- α were the inflammatory factors that were significantly increased in the serum of SAMP8 mice [18]. After 14 days of EA treatment, we found that both frequencies of EA treatment effectively reduced the four inflammatory factors. Compared with the 2 Hz EA treatment, the 10 Hz EA treatment has an advantage in reducing serum IL-1 β and IL-6 levels. Cognitive function is critically related to the hippocampal CA1 and CA3 regions, which were observed in this study [18]. Compared with the hippocampus of SAMR1 mice, we found that those of SAMP8 mice exhibited a disordered pyramidal cell arrangement, incomplete membrane structure, shrinking nuclei, and other abnormal pathological findings, which was consistent with most previous reports using SAMP8 mice as model animals. More importantly, we found that EA, especially the 10 Hz EA treatment, can effectively improve these typical pathological changes, which are more obvious.

Hippocampal TUNEL staining and quantitative analysis are common detection methods conducted on the death of neurons. Compared with SAMR1 mice, SAMP8 mice were characterized by increased numbers and ratios of TUNEL-positive cells in the hippocampal CA1 and CA3 regions.

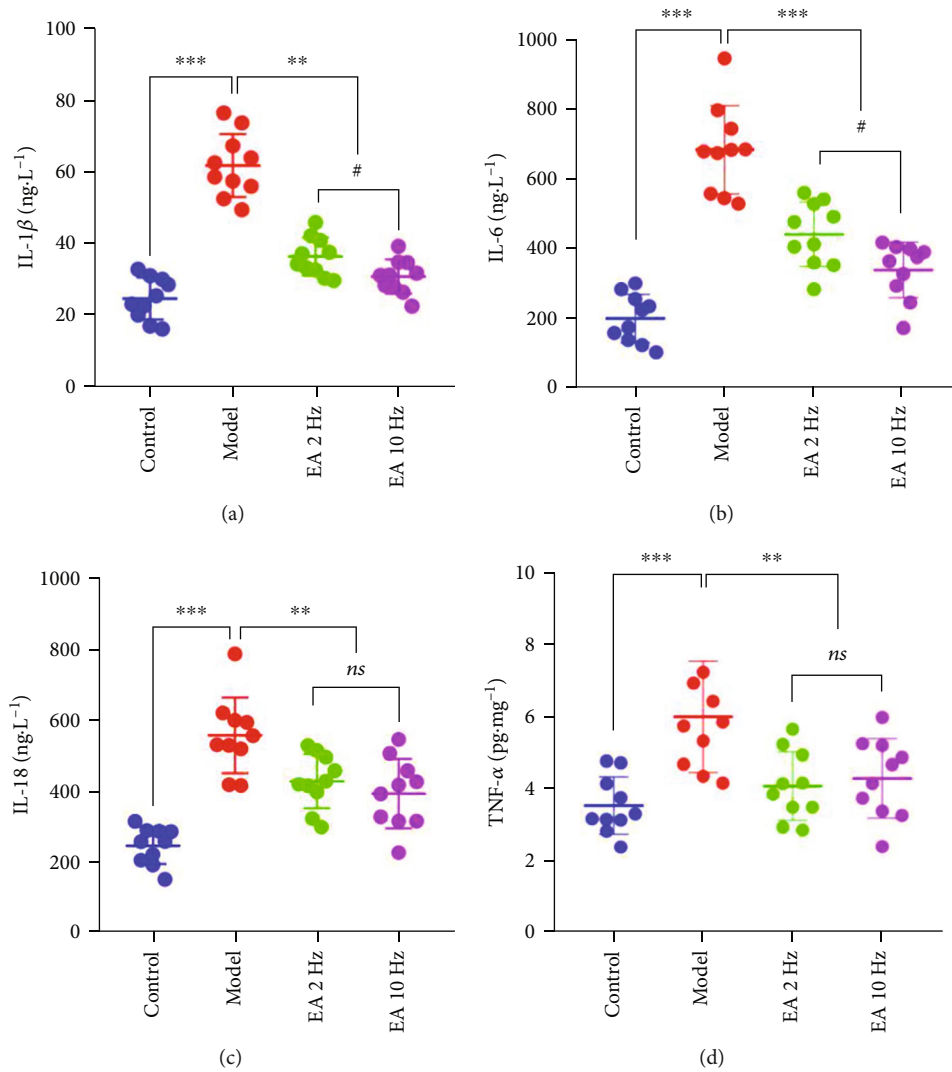


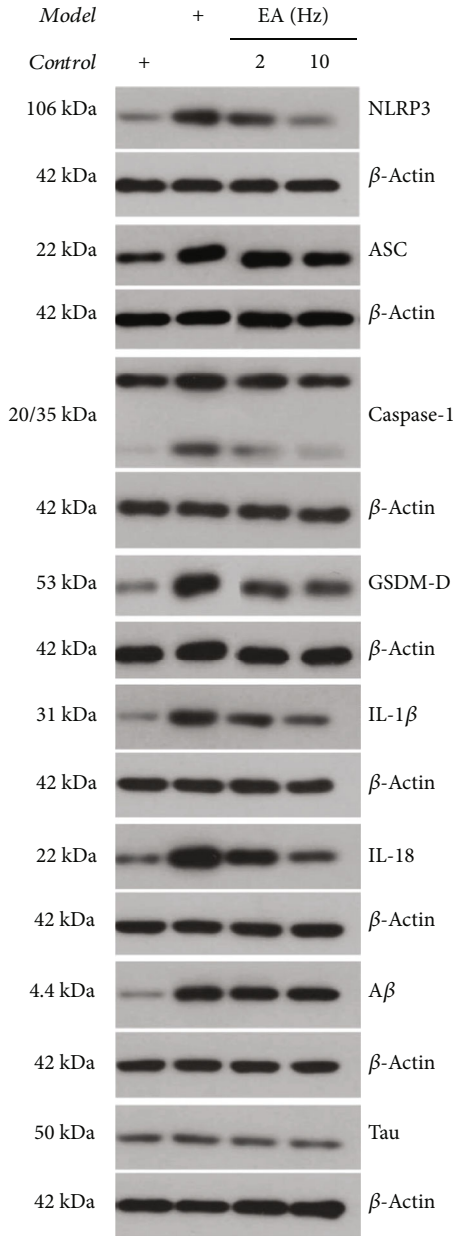
FIGURE 5: Electroacupuncture (EA) treatment attenuated the serum inflammatory factors in SAMP8 mice. (a) The level of interleukin-1 β (IL-1 β). (b) The level of interleukin-6 (IL-6). (c) The level of interleukin-18 (IL-18). (d) The level of tumor necrosis factor α (TNF- α). Data are presented as the means \pm standard error of the mean ($n = 10$ per group). *** $P < 0.001$ and ** $P < 0.01$ vs. the model group; # $P < 0.05$ vs. the 2 Hz EA group. ns: not significant.

The model mouse hippocampus may have neuronal cell death induced by inflammation, and this mode of cell death has been the focus area of CI in recent years. After 14 days of EA treatment, we found that EA could effectively reverse the cell death and the ratio of TUNEL-positive neurons in the hippocampal CA1 and CA3 regions and that 10 Hz EA treatment had a more significant reversal effect on the CA1 region than 2 Hz EA treatment. Furthermore, the increase in EA frequency may play a better role in inhibiting inflammation and hippocampal cell death.

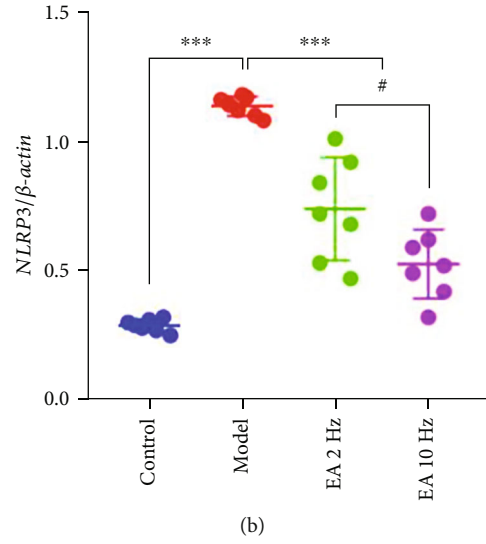
4.3. High-Frequency EA Therapy Can Effectively Inhibit Hippocampal Pyroptosis through the NLRP3/Caspase-1 Pathway. At present, CI is believed to be mainly induced by abnormal changes in the tau protein framework, resulting in neurofibrillary tangles and the formation of senile plaques caused by excessive deposition of β -amyloid (β A β) [31]. In addition, various in vivo and in vitro experiments have

proven that pyroptosis is related to the pathogenesis of CI [5, 32], but the specific mechanism by which it participates remains unclear. The inflammatory response is a protective mechanism initiated by immune cells in response to injury- or infection-related factors; meanwhile, a long-term excessive inflammatory response may aggravate neural plasticity damage and disease progression. The neuroinflammatory response is generally believed to be regulated by NLRP3 inflammasome-dependent pyroptosis of neurons, and the death of neurons caused by pyroptosis is closely related to the onset of cognitive impairment [33].

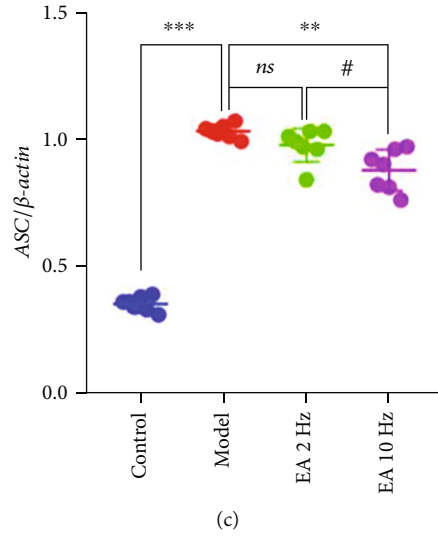
The NLRP3 inflammasome comprises NLRP3, ASC, and caspase-1 [34]. GSDM-D (gasdermin-d) is the substrate of caspase-1 [35]. After GSDM-D protein is activated by caspase-1, it can cause cell membrane rupture, allowing water molecules and other substances to enter cells [36]; it can thereby induce the release of a large number of inflammatory cytokines, including IL-1 β and IL-18, causing cell pyroptosis



(a)



(b)



(c)

FIGURE 6: Continued.

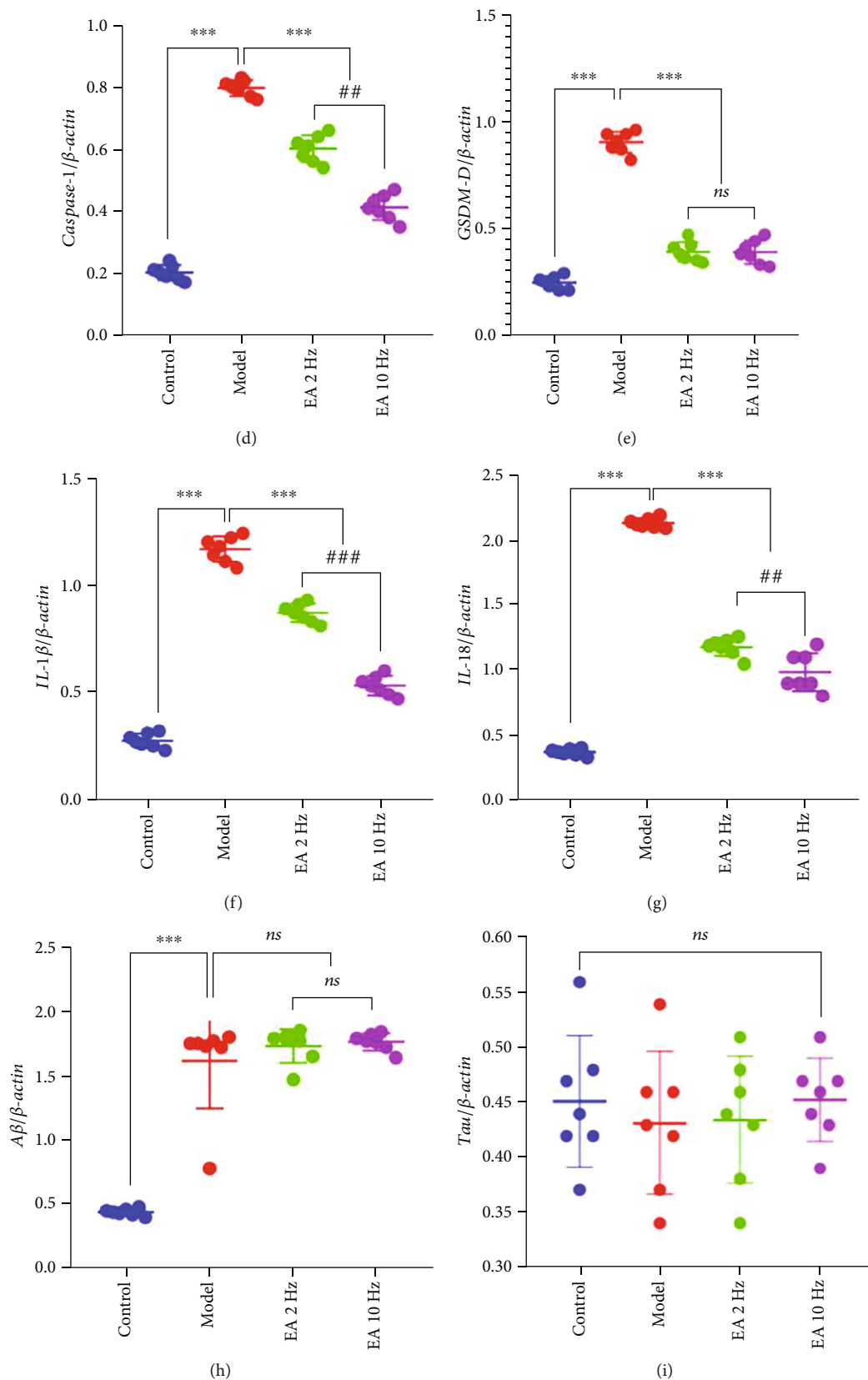


FIGURE 6: Expression of NLRP3/caspase-1 signaling-related proteins in the hippocampal tissue. (a) Western blot images showing the protein levels of NLRP3, ASC, caspase-1, GSDM-D, IL-1 β , IL-18, A β , and tau in the hippocampus. (b-i) Quantification of NLRP3, ASC, caspase-1, GSDM-D, IL-1 β , IL-18, A β , and tau bands in the hippocampus. Data are presented as the means \pm standard error of the mean ($n = 7$ per group). *** $P < 0.001$ vs. the model group, ### $P < 0.001$ and ## $P < 0.01$ vs. the 2 Hz EA group. ns: not significant.

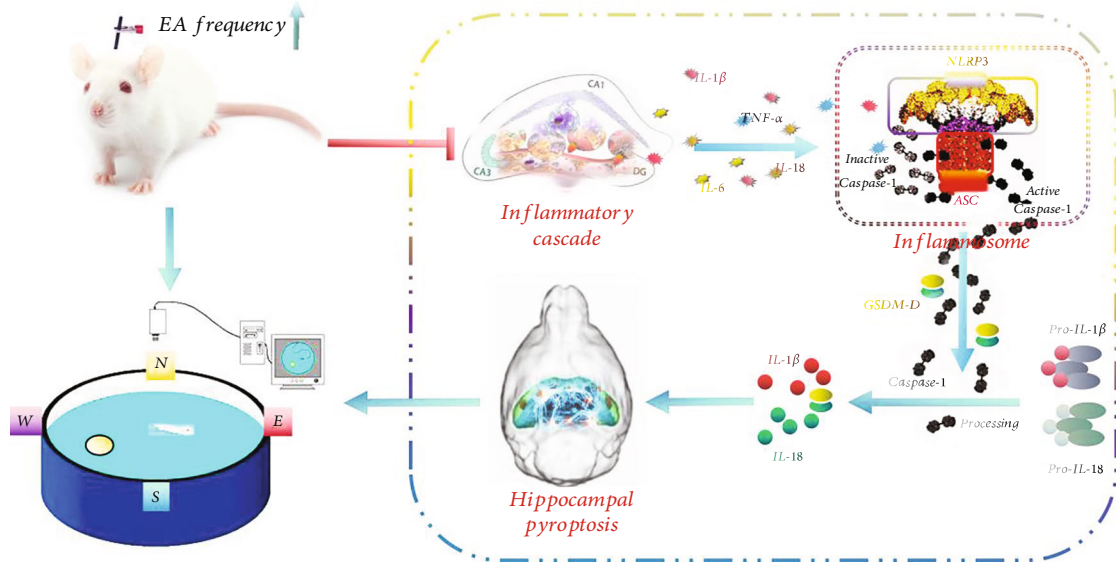


FIGURE 7: EA inhibited the activation of NLRP3 inflammasome to improve cognitive impairment. The attenuation of NLRP3 inflammasome activation ultimately reduced IL-1 β , IL-18, and GSDM-D expressions and attenuated the inflammatory response of the hippocampus, thereby inhibiting hippocampal pyroptosis to improve cognitive impairment in SAMP8 mice.

[36, 37]. Studies have shown that the NLRP3 inflammasome can identify A β and thus play an important role in the process [38]. Activated soluble interleukin-1 receptor type II, IL-18, and caspase-1 protein in cerebrospinal fluid (CSF) with mild CI and AD patients has been found by Lindberg et al. [39], indicating that inflammasome activation may be an important step in the development of early CI. Knocking out NLRP3 and caspase-1 in mouse models can largely prevent mice from developing CI-related learning and memory ability impairment and a serious pathological state [40]. Interestingly, a recent study showed that the absence of NLRP3 protected mice from aging-related inflammation and CI even in the brains of mice without excessive A β deposition [41]. Therefore, the inflammatory response dependent on NLRP3 is closely related to the cognitive decline associated with A β excessive deposition.

We found that the expression of NLRP3/caspase-1 pathway-related 6 proteins and A β protein in the hippocampus was significantly increased in SAMP8 mice compared with SAMR1 mice. Interestingly, no significant difference was found in tau protein expression, consistent with previous studies showing that extensive deposition of A β protein was a typical pathological characteristic in the hippocampal tissues of SAMP8 mice. This evidence suggests that CI in SAMP8 mice is related to NLRP3/caspase-1 pathway-mediated pyroptosis and excessive deposition of A β protein. After 14 days of EA treatment, NLRP3/caspase-1 pathway-related proteins were significantly downregulated; the 2 Hz EA treatment did not effectively reduce the expression of ASC protein, a component of the NLRP3 inflammasome, but the 10 Hz EA treatment was effective. This suggests that higher EA frequencies are more effective in inhibiting NLRP3/caspase-1 pathway-mediated cell pyroptosis (Figure 7). In other words, increasing the EA frequency can effectively inhibit hippocampal pyroptosis under the condition of acupoint determination,

and this finding has not been reported in the relevant literature yet. Our findings suggest that the frequency of EA therapy plays a crucial role in the treatment of CI, and the underlying mechanism of this phenomenon is that the inhibitory role of the inflammatory cascade-induced activation of NLRP3 inflammasome is enhanced with the increase in EA frequency within a reasonable range.

4.4. EA Could Not Reduce the A β and Tau Protein Expression of SAMP8 Mice and the Limitations of This Study. Interestingly, we found that the two common EA treatments failed to reduce the expression of A β and tau proteins in the hippocampal tissues of SAMP8 mice after 14 days. Due to the lack of high-quality reports on the mechanism of EA treatment on cognitive function in SAMP8 mice, analyzing the underlying causes is difficult. Notably, a recent report using EA treatment at the KI3 acupoint to intervene in 5XFAD mice found that EA can downregulate the expression level of A β protein [21]. We analyzed whether the failure to reduce the expression level of A β in this study may be related to acupoint selection. The reason why no significant change in tau protein was found may be related to the absence of such pathological characteristics in the SAMP8 model mice.

The limitations of this study are as follows. First, acupoint specificity is the main factor influencing acupuncture outcomes in clinical and animal studies. Whether EA at the GV20 and ST36 acupoints is the best choice or whether EA at other acupoints improves cognitive function in SAMP8 mice with CI through the restoration of the NLRP3/caspase-1 signaling pathway needs to be further explored. Second, acupuncture has bidirectional regulatory effects under different functional conditions; thus, a follow-up is necessary for conducting EA research on the changes in mouse electroencephalogram (EEG). Third, previous studies have found that pyroptosis occurs faster than other forms of cell death,

such as apoptosis. The acupoint ST36 is on the leg, and the GV 20 acupoint is on the head. How the exact pathways that transduce the EA signal at two relatively distant acupoints to the hippocampus to affect protein translation in the animal model needs further exploration.

5. Conclusion

In conclusion, the present study provides evidence that EA treatment improves cognitive function, reduces inflammation, and inhibits pyroptosis in SAMP8 mice. The inhibition of NLRP3/caspase-1 signaling in the hippocampus may be involved in the beneficial effect of EA treatment on cognitive function.

Data Availability

The data used to support the findings of this study are available from the corresponding author upon request.

Conflicts of Interest

The authors declare that no conflicts of interest exist regarding the publication of this paper.

Authors' Contributions

Zhongren Sun, Jing Chen, and Hongcai Shang designed the experiments. Zhitao Hou, Meng Wang, Tingting Mei, Yue Zhang, Liying Song, and Xianming Shao performed the experiments. Ruijin Qiu, Qingshuang Wei, and Yitian Liu analyzed the data and revised the manuscript. All authors discussed the results and commented on the manuscript. All authors approved the final version of manuscript for submission. Zhitao Hou and Ruijin Qiu contributed equally to this work.

Acknowledgments

This work was supported by the National Natural Sciences Foundation of China (Grant No. 81904307), the Natural Science Foundation of Heilongjiang University of Chinese Medicine (Grant No. 201838), and the Young and Middle-aged Teachers Scientific Research Project of Heilongjiang University of Chinese Medicine (Grant No. 2017001).

References

- [1] G. S. Vlachos, M. H. Kosmidis, M. Yannakoulia et al., "Prevalence of mild cognitive impairment in the elderly population in Greece: results from the HELIAD study," *Alzheimer Disease & Associated Disorders*, vol. 34, no. 2, pp. 156–162, 2020.
- [2] D. Seblova, C. Brayne, V. Machu, M. Kuklova, M. Kopecek, and P. Cermakova, "Changes in cognitive impairment in the Czech Republic," *Journal of Alzheimer's Disease*, vol. 72, no. 3, pp. 693–701, 2019.
- [3] E. X. Wei, E. S. Oh, A. Harun et al., "Increased prevalence of vestibular loss in mild cognitive impairment and Alzheimer's disease," *Current Alzheimer Research*, vol. 16, no. 12, pp. 1143–1150, 2019.
- [4] M. Overton, M. Pihlgard, and S. Elmstahl, "Prevalence and incidence of mild cognitive impairment across subtypes, age, and sex," *Dementia and Geriatric Cognitive Disorders*, vol. 47, no. 4–6, pp. 219–232, 2019.
- [5] L. Yin, F. Bao, J. Wu, and K. Li, "NLRP3 inflammasome-dependent pyroptosis is proposed to be involved in the mechanism of age-dependent isoflurane-induced cognitive impairment," *Journal of Neuroinflammation*, vol. 15, no. 1, p. 266, 2018.
- [6] Q. Fu, J. Li, L. Qiu et al., "Inhibiting NLRP3 inflammasome with MCC950 ameliorates perioperative neurocognitive disorders, suppressing neuroinflammation in the hippocampus in aged mice," *International Immunopharmacology*, vol. 82, p. 106317, 2020.
- [7] Y. Fan, L. Du, Q. Fu et al., "Inhibiting the NLRP3 Inflammasome with MCC950 ameliorates isoflurane-induced pyroptosis and cognitive impairment in aged mice," *Frontiers in Cellular Neuroscience*, vol. 12, p. 426, 2018.
- [8] R. Zhou, X. Yang, X. Li et al., "Recombinant CC16 inhibits NLRP3/caspase-1-induced pyroptosis through p38 MAPK and ERK signaling pathways in the brain of a neonatal rat model with sepsis," *Journal of Neuroinflammation*, vol. 16, no. 1, p. 239, 2019.
- [9] K. Tsuchiya, "Inflammasome-associated cell death: pyroptosis, apoptosis, and physiological implications," *Microbiology and Immunology*, vol. 64, no. 4, pp. 252–269, 2020.
- [10] W. Gong, Y. Shi, and J. Ren, "Research progresses of molecular mechanism of pyroptosis and its related diseases," *Immunobiology*, vol. 225, no. 2, article 151884, 2020.
- [11] Z. Yang, C. Liang, T. Wang et al., "NLRP3 inflammasome activation promotes the development of allergic rhinitis via epithelium pyroptosis," *Biochemical and Biophysical Research Communications*, vol. 522, no. 1, pp. 61–67, 2020.
- [12] G. Wang, T. Shen, P. Li et al., "The increase in IL-1 β in the early stage of heatstroke might be caused by splenic lymphocyte pyroptosis induced by mtROS-mediated activation of the NLRP3 inflammasome," *Frontiers in Immunology*, vol. 10, p. 2862, 2019.
- [13] V. Elce, A. Del Pizzo, E. Nigro et al., "Impact of physical activity on cognitive functions: a new field for research and management of cystic fibrosis," *Diagnostics*, vol. 10, no. 7, p. 489, 2020.
- [14] X. Li, Q. Dai, Z. Shi et al., "Clinical efficacy and safety of electroacupuncture in migraine treatment: a systematic review and network meta-analysis," *The American Journal of Chinese Medicine*, vol. 47, no. 8, pp. 1755–1780, 2019.
- [15] P. R. Lv, Y. S. Su, W. He et al., "Electroacupuncture alleviated referral hindpaw hyperalgesia via suppressing spinal long-term potentiation (LTP) in TNBS-induced colitis rats," *Neural Plasticity*, vol. 2019, 11 pages, 2019.
- [16] J. Du, J. Fang, C. Wen, X. Shao, Y. Liang, and J. Fang, "The effect of electroacupuncture on PKMzeta in the ACC in regulating anxiety-like behaviors in rats experiencing chronic inflammatory pain," *Neural Plasticity*, vol. 2017, Article ID 3728752, 13 pages, 2017.
- [17] X. Wang, Z. Li, C. Li, Y. Wang, S. Yu, and L. Ren, "Electroacupuncture with Bushen Jiannao improves cognitive deficits in senescence-accelerated mouse prone 8 mice by inhibiting neuroinflammation," *Journal of Traditional Chinese Medicine*, vol. 40, no. 5, pp. 812–819, 2020.
- [18] Z. Hou, F. Li, J. Chen et al., "Beneficial effects of sagacious Confucius' pillow elixir on cognitive function in senescence-

- accelerated P8 mice (SAMP8) via the NLRP3/caspase-1 pathway," *Evidence-Based Complementary and Alternative Medicine*, vol. 2019, Article ID 3097923, 13 pages, 2019.
- [19] Z. Hou, Z. Sun, and S. Sun, "Impacts of the repetitive transcranial acupuncture stimulation on the content of serum orexin A in patients with post-stroke insomnia," *Zhongguo Zhen Jiu*, vol. 38, no. 10, pp. 1039–1042, 2018.
- [20] Z. T. Hou, Z. R. Sun, S. T. Liu et al., "Effects of electroacupuncture intervention on oxygen free radicals and expression of apoptosis-related proteins in rats with ischemic learning and memory disorder," *Zhen Ci Yan Jiu*, vol. 40, no. 6, pp. 431–438, 2015.
- [21] M. Cai, J. H. Lee, and E. J. Yang, "Electroacupuncture attenuates cognition impairment via anti-neuroinflammation in an Alzheimer's disease animal model," *Journal of Neuroinflammation*, vol. 16, no. 1, p. 264, 2019.
- [22] R. Lin, J. Huang, J. Xu et al., "Effect and neuroimaging mechanism of electroacupuncture for vascular cognitive impairment no dementia: study protocol for a randomized, assessor-blind, controlled clinical trial," *Evidence-based Complementary and Alternative Medicine*, vol. 2020, Article ID 7190495, 8 pages, 2020.
- [23] J. H. Kim, J. Y. Han, G. C. Park, and J. S. Lee, "Effects of electroacupuncture combined with computer-based cognitive rehabilitation on mild cognitive impairment: study protocol for a pilot randomized controlled trial," *Trials*, vol. 20, no. 1, p. 478, 2019.
- [24] Y. G. Han, X. Qin, T. Zhang et al., "Electroacupuncture prevents cognitive impairment induced by lipopolysaccharide via inhibition of oxidative stress and neuroinflammation," *Neuroscience Letters*, vol. 683, pp. 190–195, 2018.
- [25] H. Xu, Y. M. Zhang, H. Sun, S. H. Chen, and Y. K. Si, "Electroacupuncture at GV20 and ST36 exerts neuroprotective effects via the EPO-mediated JAK2/STAT3 pathway in cerebral ischemic rats," *Evidence-based Complementary and Alternative Medicine*, vol. 2017, Article ID 6027421, 11 pages, 2017.
- [26] J. W. Yang, X. R. Wang, S. M. Ma, N. N. Yang, Q. Q. Li, and C. Z. Liu, "Acupuncture attenuates cognitive impairment, oxidative stress and NF- κ B activation in cerebral multi-infarct rats," *Acupuncture in Medicine*, vol. 37, no. 5, pp. 283–291, 2019.
- [27] K. Chan, L. Lui, K. Yu et al., "The efficacy and safety of electroacupuncture for alleviating chemotherapy-induced peripheral neuropathy in patients with colorectal cancer: study protocol for a single-blinded, randomized sham-controlled trial," *Trials*, vol. 21, no. 1, p. 58, 2020.
- [28] H. Jin, Y. Xiang, Y. Feng et al., "Effectiveness and safety of acupuncture moxibustion therapy used in breast cancer-related lymphedema: a systematic review and meta-analysis," *Evidence-based Complementary and Alternative Medicine*, vol. 2020, Article ID 3237451, 10 pages, 2020.
- [29] J. Jiang, G. Liu, S. Shi, and Z. Li, "Musical electroacupuncture may be a better choice than electroacupuncture in a mouse model of Alzheimer's disease," *Neural Plasticity*, vol. 2016, Article ID 3131586, 9 pages, 2016.
- [30] E. M. Rhea, S. Nirkhe, S. Nguyen et al., "Molecular mechanisms of intranasal insulin in SAMP8 mice," *Journal of Alzheimer's Disease*, vol. 71, no. 4, pp. 1361–1373, 2019.
- [31] S. L. Garrett, D. McDaniel, M. Obideen et al., "Racial disparity in cerebrospinal fluid Amyloid and tau biomarkers and associated cutoffs for mild cognitive impairment," *JAMA Network Open*, vol. 2, no. 12, p. e1917363, 2019.
- [32] S. Zhu, Z. Zhang, L. Q. Jia et al., "Valproic acid attenuates global cerebral ischemia/reperfusion injury in gerbils via anti-pyroptosis pathways," *Neurochemistry International*, vol. 124, pp. 141–151, 2019.
- [33] H. G. Ding, Y. Y. Deng, R. Q. Yang et al., "Hypercapnia induces IL-1 β overproduction via activation of NLRP3 inflammasome: implication in cognitive impairment in hypoxemic adult rats," *Journal of Neuroinflammation*, vol. 15, no. 1, p. 4, 2018.
- [34] C. Y. Hsieh, L. H. Li, Y. Lam et al., "Synthetic 4-hydroxy auxarconjugatin B, a novel Autophagy inducer, attenuates gouty inflammation by inhibiting the NLRP3 inflammasome," *Cells*, vol. 9, no. 2, p. 279, 2020.
- [35] H. Dubois, F. Sorgeloos, S. T. Sarvestani et al., "Nlrp3 inflammasome activation and Gasdermin D-driven pyroptosis are immunopathogenic upon gastrointestinal norovirus infection," *PLOS Pathogens*, vol. 15, no. 4, p. e1007709, 2019.
- [36] Q. Jiang, X. Geng, J. Warren et al., "Hypoxia inducible factor-1 α (HIF-1 α) mediates NLRP3 inflammasome-dependent-pyroptotic and apoptotic cell death following ischemic stroke," *Neuroscience*, vol. 448, pp. 126–139, 2020.
- [37] M. Adamiak, A. Ciechanowicz, M. Skoda et al., "Novel evidence that purinergic signaling - Nlrp3 inflammasome axis regulates circadian rhythm of hematopoietic stem/progenitor cells circulation in peripheral blood," *Stem Cell Reviews and Reports*, vol. 16, no. 2, pp. 335–343, 2020.
- [38] A. Nakanishi, N. Kaneko, H. Takeda et al., "Amyloid β directly interacts with NLRP3 to initiate inflammasome activation: identification of an intrinsic NLRP3 ligand in a cell-free system," *Inflammation and Regeneration*, vol. 38, no. 1, 2018.
- [39] C. Lindberg, M. Chromek, L. Ahrengart, A. Brauner, M. Schultzberg, and A. Garlind, "Soluble interleukin-1 receptor type II, IL-18 and caspase-1 in mild cognitive impairment and severe Alzheimer's disease," *Neurochemistry International*, vol. 46, no. 7, pp. 551–557, 2005.
- [40] V. Bharti, H. Tan, H. Zhou, and J. F. Wang, "Txnip mediates glucocorticoid-activated NLRP3 inflammatory signaling in mouse microglia," *Neurochemistry International*, vol. 131, p. 104564, 2019.
- [41] B. S. Thawkar and G. Kaur, "Inhibitors of NF- κ B and P2X7/NLRP3/caspase 1 pathway in microglia: novel therapeutic opportunities in neuroinflammation induced early-stage Alzheimer's disease," *Journal of Neuroimmunology*, vol. 326, pp. 62–74, 2019.